

# SIMULATION OF THE IMPACT OF TWO-DIMENSIONAL ELASTIC DISKS

Hisao Hayakawa and Hiroto Kuninaka

*Graduate School of Human and Environmental Studies, Kyoto University,  
Sakyo-ku, Kyoto, 606-8501, Japan*

The impact of a two-dimensional elastic disk with a wall is numerically studied. It is clarified that the coefficient of restitution (COR) decreases with the impact velocity. The result is not consistent with the recent quasi-static theory of inelastic collisions even for very slow impact. The abrupt drop of COR has been found due to the plastic deformation of the disk, which is assisted by the initial internal motion. (to be published in Proceedings of 9 th Nissin Engineering Particle Technology International Symposium on 'Solids Flow Mechanics and Their Applications' held at Kyoto, 7th-9th January, 2001 )

## 1 Introduction

The collision of particles with the internal degrees of freedom are inelastic in general. The inelastic collisions are abundant in nature<sup>1</sup>. Examples can be seen in collisions of atoms, molecules, elastic materials, balls in sports, and so on. The study of inelastic collisions will be able to be widely accepted as one of fundamental subjects in physics, because they are almost always discussed in textbooks of elementary classical mechanics<sup>2</sup>.

Recent extensive interest in granular materials<sup>3</sup> makes physicists to recognize fundamental roles of inelastic collisions. In fact, granules consists of macroscopic dissipative particles. Therefore, the decision of interaction among particles is obviously important. We believe that static interactions among granular particles can be described by the theory of elasticity<sup>4, 5, 6, 7</sup>. For example, the normal compression may be described by the Hertzian contact force<sup>8</sup> and the shear force may be represented by the Mindline force<sup>9</sup>. The dynamical part related to the dissipation, however, cannot be described by any reliable physical theory. Thus, the distinct element method<sup>10</sup> which is one of the most popular models to simulate collections of granular particles contains some dynamical undetermined parameters. In other words, to determine such the parameters is important for both granular physics and fundamental physics.

The normal impact of macroscopic materials is characterized by the coefficient of restitution (COR) defined by

$$e = -v_r/v_i, \quad (1)$$

where  $v_i$  and  $v_r$  are the relative velocities of incoming and outgoing particles respectively. COR  $e$  had been believed to be a material constant, since the classical experiment by Newton<sup>11</sup>. In general, however, experiments show that COR for three dimensional materials is not a constant even in approximate sense but depends strongly on the impact velocity<sup>1, 12, 13</sup>.

The origin of the dissipation in inelastic collisions is the transfer of the kinetic energy of the center of mass into the internal degrees of freedom during the impacts. Systematic theoretical investigations of the impact have begun with the paper by Kuwabara and Kono<sup>14</sup>. Taking into account the viscous motion among the internal degrees of freedom, they derived the equation of the macroscopic deformation. Later, Brilliantov *et al.*<sup>15</sup> and Morgado and Oppenheim<sup>16</sup> derived the identical equation to eq.(2). In particular, the derivation by Morgado and Oppenheim<sup>16</sup> is based on the standard technique of nonequilibrium statistical mechanics to extract the slow mode among the fast many modes which can be regarded as the thermal reservoir. Furthermore, Brilliantov *et al.* compared their theoretical results with experimental results<sup>17</sup>. Thus, the quasi-static theory has been accepted as reasonable one.

On the other hand, Gerl and Zippelius<sup>18</sup> performed the microscopic simulation of the two-dimensional collision of an elastic disk with a wall. Their simulation is mainly based on the mode expansion of an elastic disk under the force free boundary condition. Then, they solve Hamilton's equation determined by the elastic field and the repulsive potential to represent the collision of two disks. Their results show that COR decreases with the impact velocity, which strongly depends on Poisson's ratio. For high velocity of the impact they demonstrate the macroscopic deformation has left after the collision is over. Although it is not easy to discuss the impact with the very low impact velocity from their method, their analysis may suggest the possibility of a complicated relation between the quasi-static theory of impact<sup>14, 15, 16</sup> and their microscopic simulation<sup>18</sup>. Thus, we have to clarify the relation between two typical approaches.

In this paper, we will perform the microscopic simulation of the impact of a two dimensional elastic disk with a wall. We introduce two methods of simulation; One is based on the lattice model (model A) and another is continuum model (model B) which is identical to that by Gerl and Zippelius<sup>18</sup>. Through our simulation, we will demonstrate that (i) the effect of temperature (the initial internal motion) is important, (ii) COR is suddenly dropped by the plastic deformation which is enhanced by the initial temperature, and (iii) the continuum model (model B) does not recover the results predicted by the quasi-static theories in the low impact velocity<sup>14, 15, 16</sup>.

The organization of this paper is as follows. In the next section, we will briefly review the outline of quasi-static theory<sup>14, 15, 16</sup>. In section 3, we will explain model A and model B which is equivalent to the model by Gerl and Zippelius<sup>18</sup> of our simulation. In section 4, we will show the result of our simulation and discuss the validity of quasi-static theory. In section 5, we discuss our results, in particular, about the plastic deformation by the impact and its origin. In section 6, we will summarize our result.

## 2 Quasi-static theory

In this section, we briefly explain the outline of quasi-static theory. One purpose of this section is to summarize the two-dimensional version of quasi-static theory which may not be mentioned in any articles explicitly.

At first, let us summarize the three dimensional result, in which the equation of the macroscopic deformation is given by

$$\ddot{h} = -kh^{3/2} - \gamma\sqrt{h}\dot{h} \quad (2)$$

in a collision of two spheres, where the macroscopic deformation  $h$  is given by  $h = R_1 + R_2 - |\mathbf{r}_1 - \mathbf{r}_2|$  with the radius  $R_i (i = 1, 2)$  and the position of the center of the mass  $\mathbf{r}_i$  of  $i$  th particle.  $\dot{h}$  and  $\ddot{h}$  are respectively  $dh/dt$  and  $d^2h/dt^2$ .  $k$  and  $\gamma$  are unimportant constants. The first term of the right hand side in eq.(2) represents the Hertzian contact force<sup>4, 5, 6, 8</sup> and the second term is the dissipation due to the internal motion.

The simplest derivation of eq.(2) is that by Brilliantov *et al.*<sup>15</sup>, though we also check it validity by the alternative methods. Taking into account the limitation of the length of this paper, we follow the argument by them.

The static stress tensor in the two-dimensional linear elastic material can be represented by

$$\sigma^{(el)}_{ij} = 2\mu(\epsilon_{ij} - \delta_{ij}\epsilon_{ll}/2) + K\delta_{ij}\epsilon_{ll} \quad (3)$$

where  $\mu$  and  $K$  are respectively the shear modulus and the compressional modulus, and  $\epsilon_{ij}$  is given by

$$\epsilon_{ij} = \frac{1}{2} \left( \frac{\partial u_i}{\partial x_j} + \frac{\partial u_j}{\partial x_i} \right) \quad (4)$$

with the displacement field  $u_i$ .

The two dimensional Hertzian contact law<sup>6, 18</sup> is given by the relation between the macroscopic deformation of the center of mass  $h$  and the elastic force  $F_{el}$  as

$$h \simeq -\frac{F_{el}}{\pi Y} \left\{ \ln \left( \frac{4\pi Y R}{F_{el}(1 - \sigma^2)} \right) - 1 \right\}, \quad (5)$$

where  $Y$ ,  $\sigma$  and  $R$  are the Young modulus, Poisson's ratio and the radius of the disk without deformation, respectively. Equation (5) can be derived from the stress tensor (3) with the standard treatment of linear elastic theory. Note that  $h$  satisfies  $h = R - y_0$  with the position of the center of mass  $y_0$ <sup>18</sup>.

For small dissipation, as in the textbooks<sup>5</sup>, the dissipative stress tensor due to the viscous motion among internal motions is given by

$$\sigma^{(vis)}_{ij} = 2\eta_1(\dot{\epsilon}_{ij} - \delta_{ij}\dot{\epsilon}_{ll}/2) + \eta_2\delta_{ij}\dot{\epsilon}_{ll} \quad (6)$$

as in the case of viscous fluid, where  $\dot{\epsilon}_{ij}$  is the time derivative of  $\epsilon_{ij}$ ,  $\eta_i$  ( $i = 1, 2$ ) is the viscous constant.

Brilliantov *et al.*<sup>15</sup> assumed that the velocity of deformation field is governed by the macroscopic deformation, *i.e.*,  $\dot{u}_i \simeq \dot{h}(\partial u_i / \partial h)$ . Since in the limit of  $v_i \rightarrow 0$  we

may replace eq.(5) by  $F_{el} \simeq -\pi Yh / \ln(4R/h)^{18}$ . Thus, with the aid of the assumption by Brilliantov *et al.*<sup>15</sup>, (3) and (6), it is easy to derive the two dimensional version of quasi-static theory as

$$F_{tot} \simeq -\frac{\pi Yh}{\ln(4R/h)} - A \frac{\pi Y \dot{h}}{\ln(4R/h)}, \quad (7)$$

where  $A$  is an unimportant constant. This result can be derived by various other method. Thus, we will compare the result of our simulation with eq.(7).

### 3 Our models

Let us explain the details of our model. In both models, the wall exists at  $y = 0$ , and the center of mass keeps the position at  $x = 0$ . The disk approaches from  $y > 0$  region and is rebounded by the wall.

#### 3.1 Model A

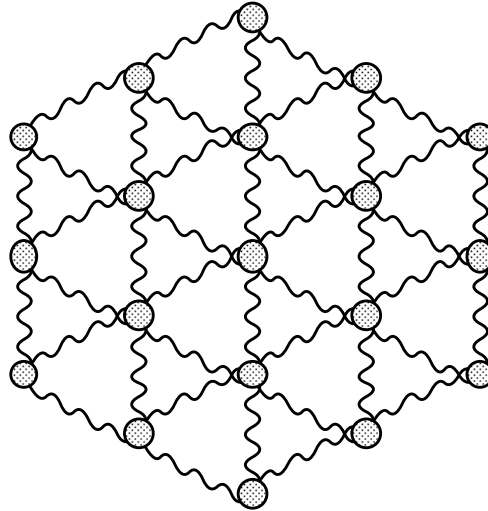


Figure 1: A schematic figure of a disk used in model A.

The disk in model A consists of some mass points (with the mass  $m$ ) on the triangular lattice. All the mass points are combined with linear springs with the spring constant  $\kappa$ . In the limit of large number of the mass points, this disk corresponds to the continuum circular disk with the Young's modulus  $Y = 2\kappa/\sqrt{3}$  and Poisson's ratio  $1/3^{19}$ . The position of each mass point of model A is governed by the following equation:

$$m \frac{d^2 \mathbf{r}_p}{dt^2} = -\kappa \sum_{i=1}^6 (d_0 - |\mathbf{r}_p - \mathbf{r}_i|) \frac{\mathbf{r}_p - \mathbf{r}_i}{|\mathbf{r}_p - \mathbf{r}_i|} + \hat{y} a V_0 e^{-ay_p} \quad (8)$$

where  $d_0$  is the lattice constant,  $\mathbf{r}_i$  is the position of the nearest neighbor mass points of  $\mathbf{r}_p$ ,  $m$  is the mass of the mass points,  $y_p$  is the  $y$  coordinate of  $\mathbf{r}_p$ , and  $\hat{y}$  is the unit vector of  $y$  direction. Note that the directional projection of the linear spring force in model A can cause the nonlinear deformation. The wall potential is given by  $V_0 e^{-ay}$ , where  $V_0 = a/2$  and  $a = 100/d_0$  for model A. The number of the mass points is fixed to 1459 in model A, since the rough evaluation of convergence of the results has been checked in this model.

### 3.2 Model B

In this subsection, we introduce model B which is originally proposed by Gerl and Zippelius<sup>18</sup>. Although the details of this model can be checked in their paper, we present the minimum description of this model to understand the setup of our simulation.

Gerl and Zippelius<sup>18</sup> analyze Hamilton's equation ;

$$\dot{P}_{n,l} = -\frac{\partial H}{\partial Q_{n,l}}; \quad \dot{Q}_{n,l} = \frac{\partial H}{\partial P_{n,l}} \quad (9)$$

under the Hamiltonian

$$H = \frac{p_0^2}{2M} + \sum_{n,l}^N \left( \frac{P_{n,l}^2}{2M} + 12M\omega_{n,l}^2 Q_{n,l}^2 \right) + V_0 \int_{-\pi/2}^{\pi/2} d\phi e^{-ay(\phi,t)}. \quad (10)$$

Here  $Q_{n,l}$  is the expansion coefficient of the 2D elastic deformation field in the polar coordinate  $\mathbf{u} = (u_r, u_\phi)$

$$(u_r(r, \phi), u_\phi(r, \phi)) = \sum_{n,l} Q_{n,l} (u_r^{n,l}(r) \cos n\phi, u_\phi^{n,l}(r) \sin n\phi), \quad (11)$$

where  $u_r^{n,l}(r)R = A_{n,l} \frac{dJ_n(k_{n,l}r)}{dr} + nB_{n,l} \frac{J_n(k_{n,l}r)}{r}$  and  $u_\phi^{n,l}(r)R = -nA_{n,l} \frac{J_n(k_{n,l}r)}{r} - B_{n,l} \frac{dJ_n(k_{n,l}r)}{dr}$  with the radius of the disk and the Bessel function of the  $n$ -th order  $J_n(x)$ . Here  $k'_{n,l} = k_{n,l} \sqrt{2(1+\sigma)/(1-\sigma^2)}$  and  $k_{n,l}$  is the solution of

$$(1-\sigma^2)(1-n^2)\kappa\kappa'^2 J_{n-1}(\kappa)J_{n-1}(\kappa') + \kappa^2[\kappa^2 - 2n(n+1)(1-\sigma)]J_n(\kappa)J_n(\kappa') + (1-\sigma)[\kappa^2 - (1-\sigma)(1-n^2)n][\kappa J_{n-1}(\kappa)J_n(\kappa') + \kappa' J_{n-1}(\kappa')J_n(\kappa)] = 0 \quad (12)$$

with Poisson's ratio  $\sigma$ ,  $\kappa = k_{n,l}R$  and  $\kappa' = k'_{n,l}R$ , which is given by the boundary condition. Thus, for fixed  $n$  there are infinitely many solutions  $k_{n,l}$  and  $\omega_{n,l} = k_{n,l} \sqrt{Y/\{\rho(1-\sigma^2)\}}$  numbered by  $l = 0, 1, \dots, \infty$ .  $A_{n,l}$  and  $B_{n,l}$  are determined by

$$\begin{aligned} & -A_n \left[ \frac{(1-\sigma)}{R} \frac{dJ_n(k_{n,l}R)}{dR} + (k_{n,l}^2 - \frac{(1-\sigma)}{R^2} n^2) J_n(k_{n,l}R) \right] \\ & + nB_n(1-\sigma) \left[ \frac{1}{R} \frac{dJ_n(k'_{n,l}R)}{dR} - \frac{J_n(k'_{n,l}R)}{R^2} \right] = 0 \end{aligned} \quad (13)$$

and  $\int_0^R dr \{u_r^{n,l2} + u_\phi^{n,l2}\} = R^2$ .  $P_{n,l}$  is the canonical momentum.  $y(\phi, t)$  is the shape of the elastic disk in the polar coordinate;

$$y(\phi, t) = y_0(t) + \sum_{n,l} Q_{n,l} (C_{n,l} \cos(n\phi) \cos \phi - S_{n,l} \sin(n\phi) \sin \phi) \quad (14)$$

with the position of the center of mass  $y_0(t)$  and constants  $C_{n,l}$  and  $S_{n,l}$  determined by the maximal radial and tangential displacement at the edge of the disk as  $C_{n,l} = u_r^{n,l}(R)$  and  $S_{n,l} = u_\phi^{n,l}(R)$ .  $M$  is the mass of the disk, and the momentum of the center of the mass  $p_0 = My_0$  satisfies  $\dot{p}_0 = -(\partial H / \partial y_0)$ ,  $V_0$  and  $a$  are parameters to express the strength of the wall potential.

For the simulation of a pair of identical disks, they extrapolate the results of their simulation to  $a \rightarrow \infty$  and  $N \rightarrow \infty$  with the total number of modes  $N$ . We only adopt  $N = 1189$  ( $n \leq 50$  and  $\kappa_n \leq 50$ ) or  $N = 437$  ( $n \leq 30$  and  $\kappa_n \leq 30$ ),  $V_0 = a/2$  and  $a = 500/R$  with the radius of the disk  $R$ .

### 3.3 Parameters in both models

For the sake of simplicity and comparison between two different models, we only simulate the case of Poisson's ratio  $\sigma = 1/3$ . The numerical scheme of the integration of model A is the classical fourth order Runge-Kutta method with  $\Delta t = 1.6 \times 10^{-3} \sqrt{m/\kappa}$ . For model B, we adopt the fourth order symplectic integral method with  $\Delta t = 5.0 \times 10^{-3} R/c$  with  $c = \sqrt{Y/\rho}$  for model B where  $Y$  is Young's modulus and  $\rho$  is the density. In both models, we have checked the conservation of the total energy.

We also investigate the impact with the finite temperature. The temperature is introduced as follows: In model A, we prepare the Maxwellian for the initial velocity distribution of mass points, where the positions of all mass points are located at their equilibrium positions. From the variance of the Maxwellian we can introduce the temperature as a parameter. To perform the simulation, we prepare 10 independent samples obeying the Maxwellian with the aid of normal random number. In model B, we prepare samples in which the absolute value of each mode satisfies equipartition law exactly. The sign of each mode is assumed to be at random with the aid of the uniform random number. From the equipartition law we can introduce the temperature as a parameter of simulation, too.

The summary of differences between model A and B is as follows: (i) All of the mass points in model A interact with the wall but, in model B, only exterior boundary has the influence of the potential as in (10). (ii) Model A can have nonlinear deformations, but model B is based on the theory of linear elasticity. (iii) Model A can express some plastic deformations, but model B cannot. (iv) Model A has the six folds symmetry but model B has the rotational symmetry.

## 4 Results

Now, let us explain the details of the result of our simulation. In the first subsection, we will introduce the result at  $T = 0$  and in the second subsection, we will show the

result at finite  $T$ .

#### 4.1 Simulation at $T = 0$

At first, we carry out the simulation of model A and model B with the initial condition at  $T = 0$  (*i.e.* no internal motion). Figure 4.1 is the plot of the COR against the impact velocity for both model A and model B. For model B, we show the results of 437 modes and 1189 modes which clearly demonstrates the convergence of the result for the number of modes. When impact velocity  $v_i$  is larger than  $0.1c$  with  $c = \sqrt{Y/\rho}$ , the value of COR of model A is almost identical to that of model B. Each line decreases smoothly as impact velocity increases. At present, we do not know the reason why the significant difference between two models exists at low impact velocity.

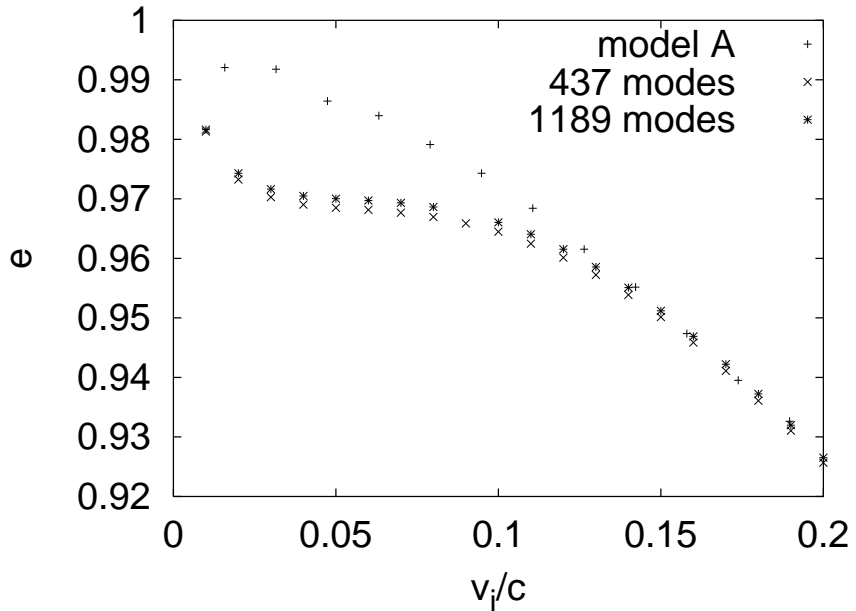


Figure 2: Coefficient of restitution for normal collision of the Model A and Model B as a function of impact velocity, where  $c = \sqrt{Y/\rho}$  with the Young's modulus  $Y$  and the density  $\rho$ .

Second, we investigate the force acting on the center of mass of the disk caused by the interaction with the wall in model B. In the limit of  $v_i \rightarrow 0$  we expect that the Hertzian contact theory can be used<sup>5, 6, 18</sup>. The small amount of transfer from the translational motion to the internal motion is the macroscopic dissipation. Thus, we can check the validity of quasi-static approaches<sup>14, 15, 16</sup> from our simulation by the difference between the observed force acting on the center of mass and the Hertzian contact force.

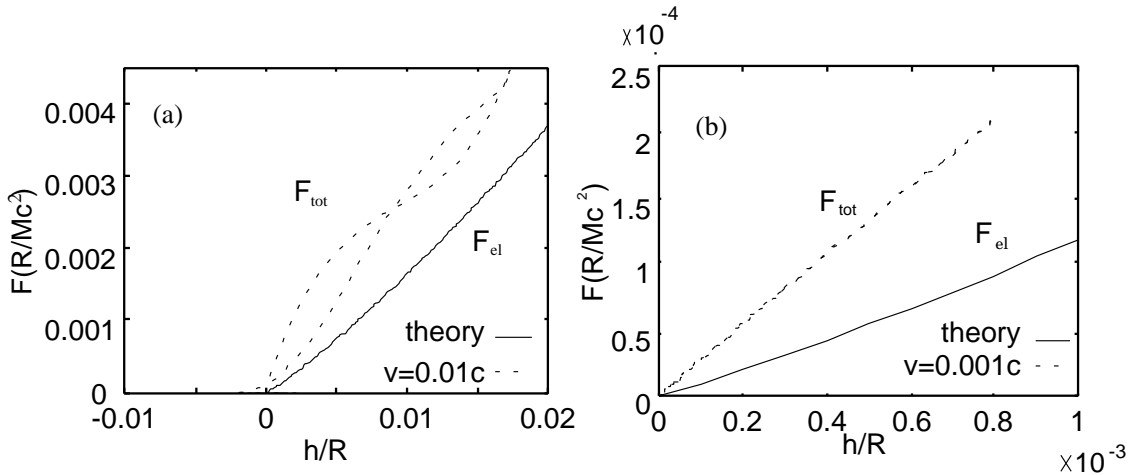


Figure 3: The comparison of the Hertzian force in eq.(5) with our simulation at  $v_i = 0.01c$  (a) and  $v_i = 0.001c$  (b) at  $T = 0$  in model B.

If  $h$  is given, we can calculate the elastic force by solving eq.(5) numerically. Figure 2 is the comparison with our simulation in model B (1189 modes) and the Hertzian contact theory (5) which is given by the solid lines. The result of our simulation at the impact velocity  $v_i = 0.01c$  with  $c = \sqrt{Y/\rho}$  shows the beautiful hysteresis as suggested in the simulation at  $v_i = 0.1c$  in ref.<sup>18</sup>. This means the compression and rebound are not symmetric. The hysteresis curve is still self-similar even at  $v_i = 0.04c$  but the loop becomes noisy at  $v_i = 0.1c$ .

For very low impact velocity  $v_i = 0.001c$ , the hysteresis loop disappears but the total force observed in our simulation is almost a linear function of  $h$  which is deviated from the Hertzian contact theory and quasi-static theory (7). In particular, the turning point at  $\dot{F} = 0$  is deviated from the Hertzian curve (the solid line). This deviation is clearly contrast to the quasi static theory, because the dissipative force in the theory in eqs.(2) and (7) must be zero at the turning point at which  $\dot{h} = 0$  should satisfy. This tendency is invariant even for the simulation of model A, though the data becomes noisy. The linearity of the total repulsion force is not surprising, because  $e^{-ay(\phi,t)}$  in the potential term in eq.(10) can be expanded by series of  $Q_{n,l}$  for very slow impact. Although we cannot judge whether the model itself is not appropriate for slow impact or the quasi-static theory is wrong, our result clearly means that the validity of the quasi-static theory cannot be supported by our microscopic simulation. However, the validity of the contact time  $\tau$  in the impact evaluated by the quasi-static theory<sup>18</sup> can be evaluated as  $\tau \simeq (\pi R/c) \sqrt{\ln(4c/v_i)}$  has been confirmed by the results of our simulation of model A (Fig.4). Thus, at least, the relation between dynamical impact theory and quasi-static elastic theory is not trivial at present.

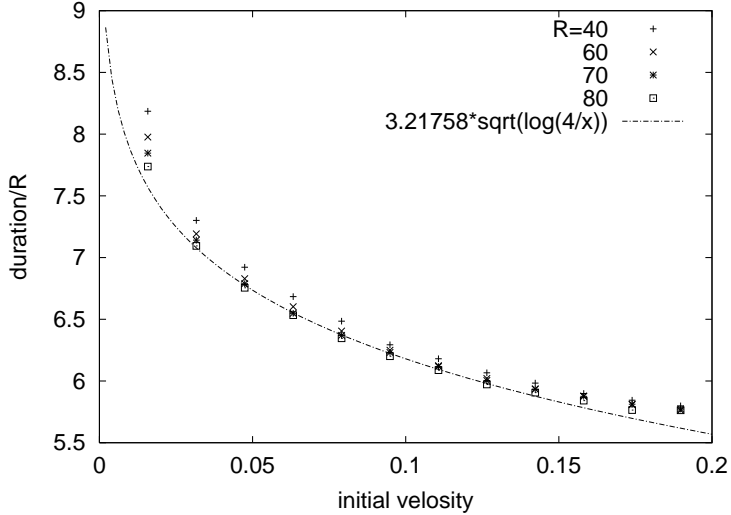


Figure 4: The plot of contact time versus the impact velocity.  $R$  represents the radius of the disk, in which  $R = 40, 60, 70$  and  $80$  correspond to the number of mass points  $5815, 13057, 17761$  and  $23233$ , respectively. The dotted line is fitting curve based on the quasi-static theory.

## 4.2 Simulation at finite $T$

Now, let us show the results of our simulation at finite  $T$  which has significant differences from those at  $T = 0$  in both low and large impact velocities. In this sense, we have much room to study this process at finite  $T$  systematically.

For small impact velocity, COR at finite  $T$  becomes larger than that at  $T = 0$  in both models. In some trials COR becomes larger than 1. It is an interesting result to extract work of this system from thermodynamical point of view. The details of the temperature effect at the slow impact will be reported elsewhere.

For large impact velocity, we do not observe any definite temperature effect in model B but we find drastic drop of COR in model A. It seems that COR can be on a universal curve when the impact velocity is scaled by the critical velocity above which COR drops abruptly (Fig.4.2). The relation between the critical velocity and the initial temperature at the intermediate impact velocities is shown in the Fig.4.2. The critical velocity seems to obey a linear function of  $T$ , though the data is not on the very slow and the very fast impacts.

## 5 discussion

We investigate what happens in the disk above the critical velocity and find the existence of plastic deformation of the disk (Fig.5(a)). Actually, there is no energy differences between two configurations in Fig.5(b) which can occur after the strong compression during the impact but cannot be released after the impact is over. It

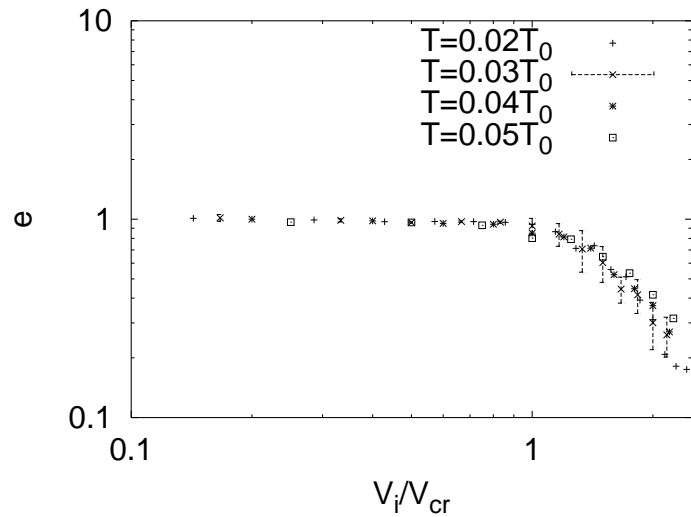


Figure 5: The relation the coefficient of restitution and the impact velocity rescaled by the critical velocity for each temperature. Curves are plotted in the log-log scale. The temperature is scaled by  $T_0 = mc^2/k_B$  with the mass of the mass points  $m$  and Boltzmann constant  $k_B$ . Note that the error bars are plotted only in the case  $T/T_0 = 0.03$  but is the same order even at other  $T$ .

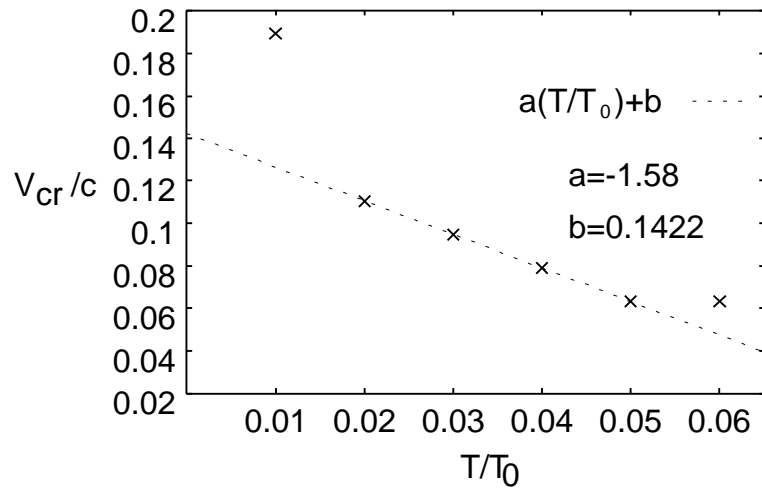


Figure 6: The plot of the initial temperature and the critical velocity causing the plastic deformation.  $v_{cr}/c = a(T/T_0) + b$  is the fitting curve line from the data between  $T/T_0 = 0.02$  and  $0.05$ .

is well known that the plastic deformation causes the drop of COR<sup>6</sup>.

Following the description in ref.6, let us explain the dimensional analysis of the two-dimensional plastic deformation. From two-dimensional Hertzian law (5) we evaluate  $h \sim a_0^2/R$  where  $a_0 = \sqrt{4F_{el}R/(\pi Y^*)}$  with the elastic force  $F_{el}$ , the radius without contact  $R$  and the effective Young's modulus  $Y^* = Y/(1-\sigma^2)$  with Poisson's ratio  $\sigma$  is the contact length in Hertzian law<sup>6</sup>. The work for the compression of the disk  $W$  is  $W = (1/2)Mv_i^2 \sim \int_0^{h^*} dh F_{el} \sim \int_0^{a_0^*} da_0 a_0/R$ , where  $M$  and  $v_i$  are the mass of the disk and the impact velocity, respectively.  $h^*$  and  $a_0^*$  are respectively the maximal compression and and the maximal contact length. Here we neglect the logarithmic correction and unimportant numerical factors. Introducing the mean contact pressure during dynamical loading  $p_d$  which satisfies  $p_d \sim F_{el}/a_0$ ,  $W$  can be evaluated by  $W \sim p_d(a_0^*)^3/R$ . From  $W \sim Mv_i^2$  we can express  $a_0^* \sim (Mv_i^2 R/p_d)^{1/3}$ .

Let us assume that the impact exceeds the yield pressure for the plastic deformation. In such the case, the deformation during rebound is frozen. Thus, the work in a rebound is  $W' \sim F_* h^*$  where  $F_*$  is the maximal force during the impact. From  $h^* \sim F_*/Y^*$  and  $F_* \sim p_d a_0^*$  we evaluate  $W' \sim (p_d a_0^*)^2/Y^*$ . Substituting the expression of  $a_0^*$  into the expression for  $W$  and  $W'$  we obtain the COR as

$$e^2 = \frac{v_r^2}{v_i^2} = \frac{W'}{W} \sim \frac{p_d^{4/3} R^{2/3}}{Y^* (M V_i^2)^{1/3}}, \quad (15)$$

where  $v_r$  is the rebound velocity. Thus, we expect the law  $e \sim v_i^{-1/3}$  in the collision of a plastic deformed disk. The three dimensional version of evaluation which gives  $e \sim v_i^{-1/4}$  agrees well with the experiment<sup>6</sup>.

Our finding is, however, something new, because (i) the drop of COR is excited by the temperature and (ii) COR decreases more rapidly like  $e \sim v_i^{-1.2}$  than that for the conventional plastic deformation  $e \sim v_i^{-1/3}$  in (15). The mechanism how to occur the plastic deformation is not clear at present including the linear law in Fig.4.2.

## 6 Conclusion

We have numerically studied the impact of a two dimensional elastic disk with the wall with the aid of model A and model B. The result can be summarized as (i) The coefficient of restitution (COR) decreases with the impact velocity. (ii) The result of our simulation is not consistent with the result of the two-dimensional quasi-static theory. For large impact velocity, there is hysteresis in the deformation of the center of mass. For small velocity, there remains the inelastic force even at  $\dot{h} = 0$ . (iii) There are drastic effects of temperature in both small and large impact velocity. (iv) In particular, for large impact velocity of model A, we have found the abrupt drop of COR above the critical impact velocity by the plastic deformation. The critical velocity of the plastic deformation seems to obey a simple linear function of temperature.

We believe that this preliminary report is meaningful to recognize that physicists have poor understanding of such the fundamental process of elementary mechanics.

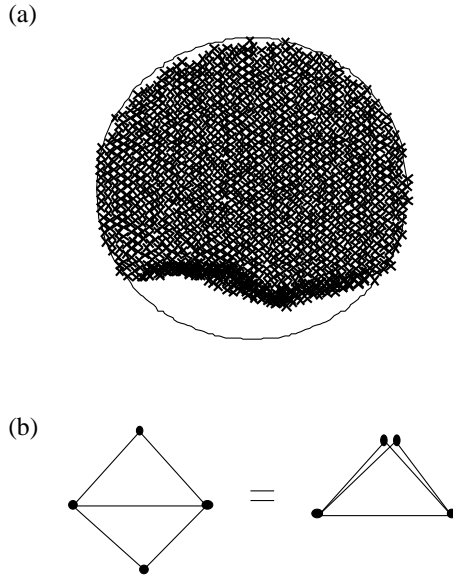


Figure 7: (a) Plastic deformation of model A with  $v_i = 0.22$  at  $T = 0.03$ . The solid circle represents the initial circle. The cross points are positions of the mass points after the collision. (b) Two configurations are energetically equivalent.

We hope that this letter will invite a lot of interest in the impact from various view points. We, at least, have a plan to study three dimensional impacts to clarify the relation among the microscopic simulation, experiments and the quasi-static elastic theory.

### Acknowledgment

We appreciate S. Sasa, S. Takesue, Y. Oono and H. Tasaki for their valuable comments. One of the authors(HK) thanks S. Wada, K. Ichiki, A. Awazu, and M. Isobe for stimulative discussions. This study is partially supported by the Grant-in-Aid for Science Research Fund from the Ministry of Education, Science and Culture (Grant No. 11740228).

### References

1. W. Goldsmith, Impact: *The Theory and Physical Behavior of Colliding Solids* (Edward Arnold Publ., London, 1960).
2. At least, the subject of inelastic collisions is always included in textbooks of physics in Japanese high schools.
3. see .e.g. L. P. Kadanoff, Rev. Mod. Phys. **71**, 435 (1999); P. G. de Gennes, *ibid*, S367 (1999) and references therein.

4. A. E. H. Love, *A Treatise on the Mathematical Theory of Elasticity* (Cambridge Univ. Press, 1927).
5. L. D. Landau and E. M. Lifshitz, *Theory of Elasticity (2nd English ed.)* (Pergamon, New York, 1960).
6. K. L. Johnson, *Contact Mechanics* (Cambridge University Press, Cambridge, 1985).
7. D. A. Hills, D. Nowell and A. Sackfield, *Mechanics of Elastic Contacts* (Butterworth-Heinemann, Oxford, 1993).
8. H. Hertz, *J. Reine Angew. Math.* **92**, 156 (1882).
9. R. D. Mindlin, *J. Appl. Mech. Trans. ASME* **16**, 259 (1949). See also ref.7.
10. P. A. Cundall and O. D. L. Strack, *Geotechnique*, **29**, 47 (1979).
11. I. Newton, *Philosophiae naturalis Principia mathematica* (W. Dawason and Sons, London, 1962). The original one has been published in 1687.
12. See, for example, R. Sondergaard, K. Chaney, and C. E. Brennen, *Transaction of the ASME, Journal of Applied Mechanics* **57**, 694 (1990); F. G. Bridges, A. Hatzes, and D.N.C. Lin, *Nature* **309**, 333 (1984); K. D. Supulver, F. G. Bridges, and D. N. C. Lin, *ICARUS* **113**, 188 (1995)
13. However, the coefficient of restitution of the collisions between one-dimensional rods does not depend on the colliding velocity but is determined by the ratio of length of the colliding rods. See ref.<sup>1</sup>. Recent studies on one-dimensional collisions can be seen in G. Giese and A. Zippelius, *Phys. Rev. E* **54**, 4828 (1996); T. Aspelmeier, G. Giese and A. Zippelius, *Phys. Rev. E* **57**, 857 (1998); A. G. Basile and R. S. Dumont, *Phys. Rev. E* **61**, 2015 (2000).
14. G. Kuwabara and K. Kono, *Jpn. J. Appl. Phys.* **26**, 1230 (1987).
15. N. Brilliantov, F. Sphan, J.-M. Hertzsch and T. Pöschel, *Phys. Rev. E* **53**, 5382 (1996).
16. W. A. Morgado and I. Oppenheim, *Phys. Rev. E* **55**, 1940 (1997).
17. e.g. T. Schwager and T. Pöschel, *Phys. Rev. E* **57**, 650 (1998); R. Ramírez, T. Pöschel, N. Brilliantov and T. Schwager, *Phys. Rev. E* **60**, 4465 (1999).
18. F. Gerl and A. Zippelius, *Phys. Rev. E* **59**, 2361 (1999).
19. W. G. Hoover, *Computational Statistical Mechanics* (Elsevier Science Publishers B. V., Amsterdam, 1991).